ACS OMEGA

http://pubs.acs.org/journal/acsodf

Article

DMTMM-Mediated Intramolecular Cyclization of Acidic Residues in Peptides/Proteins

Chi-Hua Lee, Yuan-Chao Lou, and Andrew H.-J. Wang*

Cite This: *ACS Omega* 2021, 6, 4708−4718

Read Online

ACCESS | Metrics & More | Article Recommendations | Supporting Information

ABSTRACT: The formation of succinimide in proteins has attracted considerable attention in protein aging and biopharmaceutical research. The succinimide formation occurs spontaneously in proteins and is prone to hydrolysis to yield aspartate and isoaspartate, resulting in altered protein functions. Herein, we demonstrated that the coupling reagent 4-(4,6-dimethoxy-1,3,5-triazin-2-yl)-4-methylmorpholinium chloride (DMTMM) can mediate intramolecular cyclization of aspartic acid to form succinimide efficiently in the LL37-derived short antimicrobial peptide KR12. The formation of succinimide in KR12 was confirmed by liquid chromatography tandem mass spectrometry and nuclear magnetic resonance. Moreover, the succinimide-containing KR12 displayed decreased antimicrobial activity, helicity, and serum stability in comparison with unmodified KR12. The succinimide formation usually changes the protein structure and function, and only in rare cases, it can help to maintain the protein stability. In addition to succinimide, DMTMM can also mediate intraresidue cyclization of N-terminal glutamate to form pyroglutamate. Our work thus provides a convenient and efficient method for preparation of succinimide/pyroglutamate-containing peptides, which can be used for studying their impact on peptide/protein function.

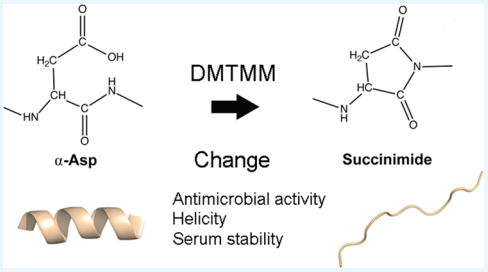

INTRODUCTION

In recent years, an increasing number of protein and peptide biopharmaceuticals have been developed for the treatment of many human diseases, such as cancer and infection.[1] Since the structure and function of peptides/proteins rely on their intrinsic feature of sequence, chemical modification is a powerful tool for alteration of peptides/proteins to improve their therapeutic efficacy.[2] However, when chemical modifications occur during storage and usage, they may cause degradation of peptides/proteins or reduction of their pharmaceutical activities.[3]

The formation of succinimide (Suc), one of the common chemical modifications of proteins, occurs spontaneously both *in vivo* and *in vitro* and may have significant effects on the biological activities of proteins.[4−7] The reactions involve a nucleophilic attack of the nitrogen atom of the following amide bond on the side chain carbonyl carbon of asparagine/aspartate (Asn/Asp), resulting in the loss of an/a ammonia/water molecule and subsequently the formation of Suc, which is prone to hydrolysis to Asp and isoAsp (Figure 1A).[4] In addition, D-Asp and D-isoAsp residues can be formed via racemization of the Suc intermediate. When the chemical modifications occur in proteins, they usually cause structural and functional alteration such as age-related protein damage in human lens and brain.[8,9] Furthermore, studies on therapeutic proteins, especially recombinant monoclonal antibodies (mAbs), have found that under mildly acidic conditions, the Suc formation is faster than its hydrolysis, resulting in accumulation of Suc.[10] Conversely, under neutral to basic conditions, hydrolysis of Suc occurs more rapidly than its formation, resulting in accumulation of Asp/isoAsp. The formation of Suc in mAbs has been shown to reduce its binding affinity.[7,11] Nevertheless, Kumar *et al.* showed that the formation of Suc helps maintain the structural stability of *Methanocaldococcus jannaschii* glutaminase.[12] Interestingly, the Suc formation is a critical step during protein splicing.[13] For biological studies and drug development, it is vital to identify the Suc formation sites and to understand the effects of Suc on peptides/proteins. However, methods for the preparation of Suc-containing peptides/proteins used in research are still limited. Since the reactions of deamidation/dehydration of Asn/Asp are non-enzymatic, they will not occur without catalyst under the physiological condition because of high energy barriers.[14,15] For this reason, the approaches for generating Suc-containing peptides/proteins usually require heat stress (≥37 °C), mildly acidic conditions (pH 4 or 5.5), and long incubation time such as a few days to months.[16−21] Moreover, the following amino acid residue in the protein sequence should be less sterically hindered such as glycine (Gly) or serine (Ser).

Received: November 11, 2020
Accepted: January 15, 2021
Published: February 5, 2021

https://dx.doi.org/10.1021/acsomega.0c05503
ACS Omega 2021, 6, 4708−4718

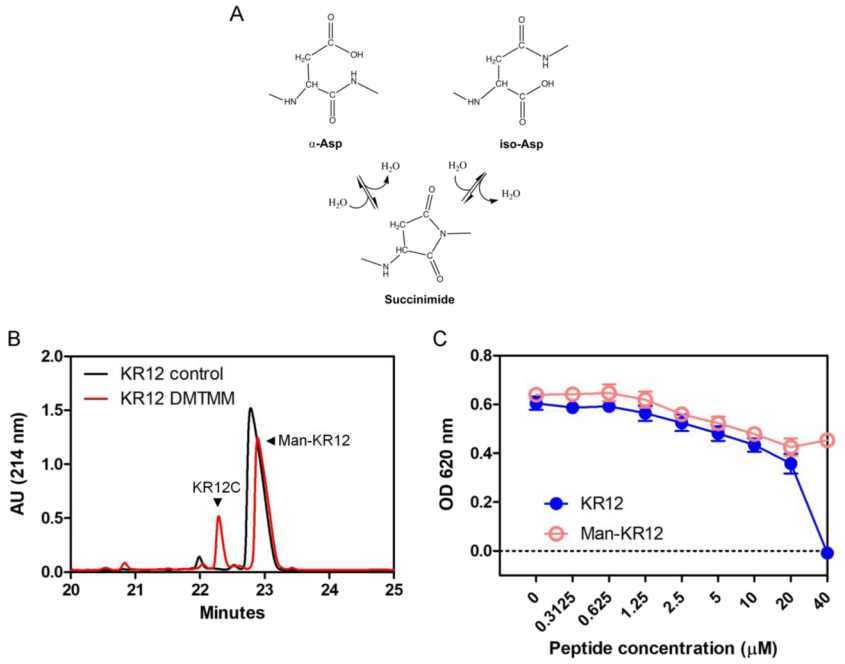

Figure 1. Mannosylation and intramolecular cyclization of KR12. (A) Mechanism of Suc formation and hydrolysis. (B) RP-HPLC profile of Man-KR12 and KR12C. (C) Antimicrobial activity of KR12 and Man-KR12 against *E. coli*. The data represent mean ± standard deviation (SD) from three independent experiments.

Antimicrobial peptides (AMPs) are regarded as promising candidates to overcome antibiotic resistance in bacteria.[22] Most of the well-known AMPs share common characteristics including a net positive charge and amphiphilicity and adopt an α-helical structure when in contact with biological membranes.[23] AMPs possess the activity to lysis cells by binding to bacterial membrane components and leading to pore formation, resulting in disruption of the membrane. LL37 belongs to the human cathelicidin family and has been isolated from degranulated neutrophils.[24] It shows broad-spectrum antimicrobial activity against Gram-positive and Gram-negative bacteria, fungi, and viruses, and it also exhibits cytotoxicity toward mammalian cells.[25] However, the length of LL37 is relatively long and thus it is unaffordable for large-scale production of the peptide. KR12 (residues 18−29 of LL37: KRIVQRIKDFLR), the smallest LL37 derivative that still possesses the antimicrobial activity, serves as a useful template for development of peptide drugs.[26]

The coupling reagent 4-(4,6-dimethoxy-1,3,5-triazin-2-yl)-4-methylmorpholinium chloride (DMTMM) has been used for condensation of carboxylic acids with amines.[27] Herein, we found that DMTMM can mediate amide bond formation between Cγ of Asp and the amine group of backbone, resulting in the formation of Suc in the peptide KR12, even though the amino acid following Asp is phenylalanine (Phe) rather than Gly or Ser. The reaction can be completed within a few hours. The Suc residue was identified by liquid chromatography tandem mass spectrometry (LC−MS/MS) and nuclear magnetic resonance (NMR). The influence of Suc on KR12 was then evaluated by comparing its antimicrobial activity, cytotoxicity, conformational changes, and serum stability with unmodified KR12. Our studies showed that the presence of Suc in KR12 significantly reduced its antimicrobial activity, helical propensity, and serum stability, whereas the substitution of Asp with glutamate (Glu), which contains similar negative charge, could increase its helical propensity and improve antimicrobial activity. Furthermore, DMTMM can also be used for intraresidue cyclization of N-terminal Glu, resulting in the formation of pyroglutamate (pGlu). The formation of pGlu in proteins, similar to Suc, has been extensively studied since they are closely associated with human disease, especially the neuropathology of Alzheimer's disease.[28] Although N-terminal pGlu is a common modification of mAbs, no evidence has shown that the pGlu formation in mAbs affects its therapeutic potency.[3,29]

RESULTS AND DISCUSSION

Conjugation of Man to KR12. Certain proteins that have the membrane-binding capability are able to disrupt cell membranes after conjugation of 4-aminophenyl-α-D-mannopyranoside (Man; Figure S1), a mannose analog, to their carboxyl groups.[30,31] Since KR12 already possesses antimicrobial activity, Man-conjugated KR12 may enhance its membrane-damaging activity, which usually positively correlates with its antimicrobial activity.[32] To generate Man-conjugated KR12 (Man-KR12), the coupling reagent DMTMM was used for conjugation of Man to the synthetic KR12 peptide under a neutral condition such as PBS (pH 7.4) or HEPES buffer (pH 7.5). There was only one carboxyl group, the side chain of Asp9, in the synthetic KR12 peptide because its C-terminal carboxyl group has been converted to amide. The mechanism involved the activation of the carboxyl group of Asp9 in KR12 by DMTMM followed by the nucleophilic attack of the amino group of Man, resulting in an amide linkage between the side chain of Asp9 and Man (Figure S1). The product after the reaction was analyzed by reversed-phase high-performance liquid chromatography (RP-HPLC) and matrix-assisted laser desorption/ionization time-of-flight/time-of-flight mass spectrometry (MALDI-TOF/TOF-MS) (Figure 1B and Figure S2). The expected molecular weight (MW) of Man-KR12 was calculated by adding the individual MW of KR12 and Man and subtracting 18 Da. The major peak

https://dx.doi.org/10.1021/acsomega.0c05503
ACS Omega 2021, 6, 4708−4718

present in HPLC after the DMTMM-coupled reaction corresponded to Man-KR12 (the observed $[M + H]^+$ = 1824.0; Table 1) The product Man-KR12 was collected and

Table 1. Calculated and Observed Monoisotopic Masses for KR12, Man-KR12, and KR12C

Peptide	Sequence	Caculated molecular mass $[M+H]^+$	Observed molecular mass $[M+H]^+$
KR12	KRIVQRIKDFLR-NH_2	1570.9	1571.0
Man-KR12	Man | KRIVQRIKDFLR-NH_2	1824.0	1824.0
KR12C	KRIVQRIKSuFLR-NH_2	1552.9	1553.0
Su : succinimide			

subjected to antimicrobial assay. The minimum inhibitory concentration (MIC) of KR12 against Gram-negative *Escherichia coli* (*E. coli*) was 40 μM. Man-KR12 displayed lower activity than KR12 (Figure 1C), indicating that conjugation of Man to KR12 reduced its antimicrobial activity.

DMTMM-Mediated Succinimide Formation. Interestingly, there was a minor peak present in RP-HPLC after the reaction, and the product (the observed $[M + H]^+$ = 1553.0; Table 1) had a mass loss of 18 Da compared to KR12 (the observed $[M + H]^+$ = 1571.0; Table 1). The product can be generated and purified by simply mixing KR12 and DMTMM in the reaction. The resulting sample was evaluated and purified by RP-HPLC before subjecting to LC−MS/MS analysis. Two fragmentation methods, higher-energy collisional dissociation (HCD) and electron transfer dissociation (ETD), were used to validate the site of modification. The HCD-MS/MS data showed that the b1 to b8 and y1 to y2 ions from all the MS^2 mass spectra were identical to the unmodified peptide of KR12, whereas the y3 to y9 showed a loss of 18 Da (Figure 2A). Moreover, the ETD-MS/MS result showed a loss of 18 Da in c_9 and $(z + 1)_4$ ions, indicating the loss of a water molecule from Asp9 (Figure 2B). These data localize the modification to the position Asp9, and the most likely modification is intraresidue cyclization/dehydration leading to the formation of a five-membered ring structure called succinimide at the position.

We then performed NMR analysis to validate the Suc formation. The ^1H resonance assignments of KR12 and KR12C at 278 K were accomplished by analyzing the two-dimensional (2D) TOCSY, NOESY, and DQF-COSY using the standard assignment procedure.[33] We identified the spin systems of residues from TOCSY and DQF-COSY and did the sequential assignment in the NOESY. The sequential connectivities between HN and Hα resonances were clearly identified by overlapping the TOCSY (blue peaks) and NOESY (red peaks) spectra of both KR12 and KR12C, as shown in Figure 3A,B, respectively. In KR12, the NOE connections from Arg2 to Arg12 were clearly assigned (Figure 3A). However, the NOE sequential connectivity of KR12C was lost at Phe10 because the HN resonance of Phe10 was missing (Figure 3B). Figure 4A shows the fingerprint region (HN-to-aliphatic protons) of TOCSY of KR12 (blue peaks) and KR12C (red peaks). The signals from Ile3 to Ile7 in both KR12 and KR12C overlapped well with each other and are indicated with black lines and labels. However, the HN signals from Lys8 to Arg12 were different between KR12 and KR12C and the most different signals were identified in Asp9 and Phe10. For Phe10, the HN signal disappeared in KR12C and the Hα and Hβ resonances identified in KR12C were remarkably different from those in KR12 (Figure 4B). For Asp9, all proton resonances in KR12 shifted significantly in KR12C, especially the HN and Hβ resonances shifted to 8.929, 3.115, and 2.619 ppm in KR12C. Based on the NMR results that HN of Phe10 vanished and other proton resonances in Asp9 and Phe10 showed significant chemical shift perturbations, we propose that in KR12C, the backbone nitrogen of Phe10 forms a covalent bond to the Cγ of Asp9 under loss of a water molecule to form Suc. The modification removes the amide proton of Phe10 but does not change the spin systems of Hα and Hβ protons in Asp9 and Phe10. Also, in a previous NMR study on Suc, the chemical shift values of HN and Hβ resonances of Suc at 298 K are 8.43, 3.25, and 2.85 ppm,[16] which are close to the values identified in KR12C at 278 K. To confirm the formation of Suc, we then analyzed all the peaks in the NOE spectra of KR12 and KR12C. Additional NOE peaks between Hα of Phe10 and Hβ of Suc were identified only in KR12C (Figure 4C). We calculated the NMR structures of KR12C based on all the NOE restraints and selected the final five structures based on the total energy. Structural superimposition of five structures on Suc9 showed that the average distance between Hα of Phe10 and Hβ of Suc9 was 4.6 Å in KR12C due to the formation of Suc (Figure 4D). NOE analysis and structure calculation confirmed the formation of Suc in KR12C.

Antimicrobial Activity and Helicity of KR12C. It has been known that the net positive charge is important for the antimicrobial activity of AMPs. The cationic AMPs interact with negatively charged bacterial cell membranes by electrostatic interactions followed by disruption of the bacterial membranes.[34] Gunasekera *et al.* found that the substitution of Asp9 in KR12 to Ala or Lys results in increased antimicrobial activity.[35] We thus performed antimicrobial activity assay to determine whether the modification of Asp9 to Suc improves antimicrobial activity due to a decrease in cationicity. However, KR12C showed decreased activity against *E. coli* in comparison with KR12 (Figure 5A). Interestingly, replacement of Asp9 to Glu in KR12, in which the charge remained unchanged, displayed a 2-fold decrease in MIC value compared to KR12, indicating that the substitution improved antimicrobial activity (Figure 5B). Besides the net charge, the ability to form a helical structure with distinct hydrophobic and hydrophilic surfaces is important for the activity of AMPs.[23] To explore the conformational behavior of KR12, KR12C, and KR12E, we performed CD experiments to observe their secondary structure after adding 2,2,2-trifluoroethanol (TFE). KR12 and KR12E formed α-helical structures after addition of TFE as indicated by negative maxima at around 208 and 222 nm and a positive maximum at around 195 nm.[36] Obviously, the helical content of KR12E was higher than that of KR12 in the presence of the same concentration of TFE (Figure 5C). In contrast, the helical content of KR12C was significantly lower than that of KR12 in 50% TFE (Figure 5D). The succinimide formation may disrupt the hydrogen bond formation between the CO group and the NH group, which is required for the helical conformation. Taken together, the results indicate that the formation of Suc in KR12 cause a decrease in α-helical propensity, which correlates well with decreased antimicrobial activity.

Cytotoxicity and Serum Stability of KR12C. Certain AMPs exhibit selective cytotoxicity toward mammalian

https://dx.doi.org/10.1021/acsomega.0c05503
ACS Omega 2021, 6, 4708−4718

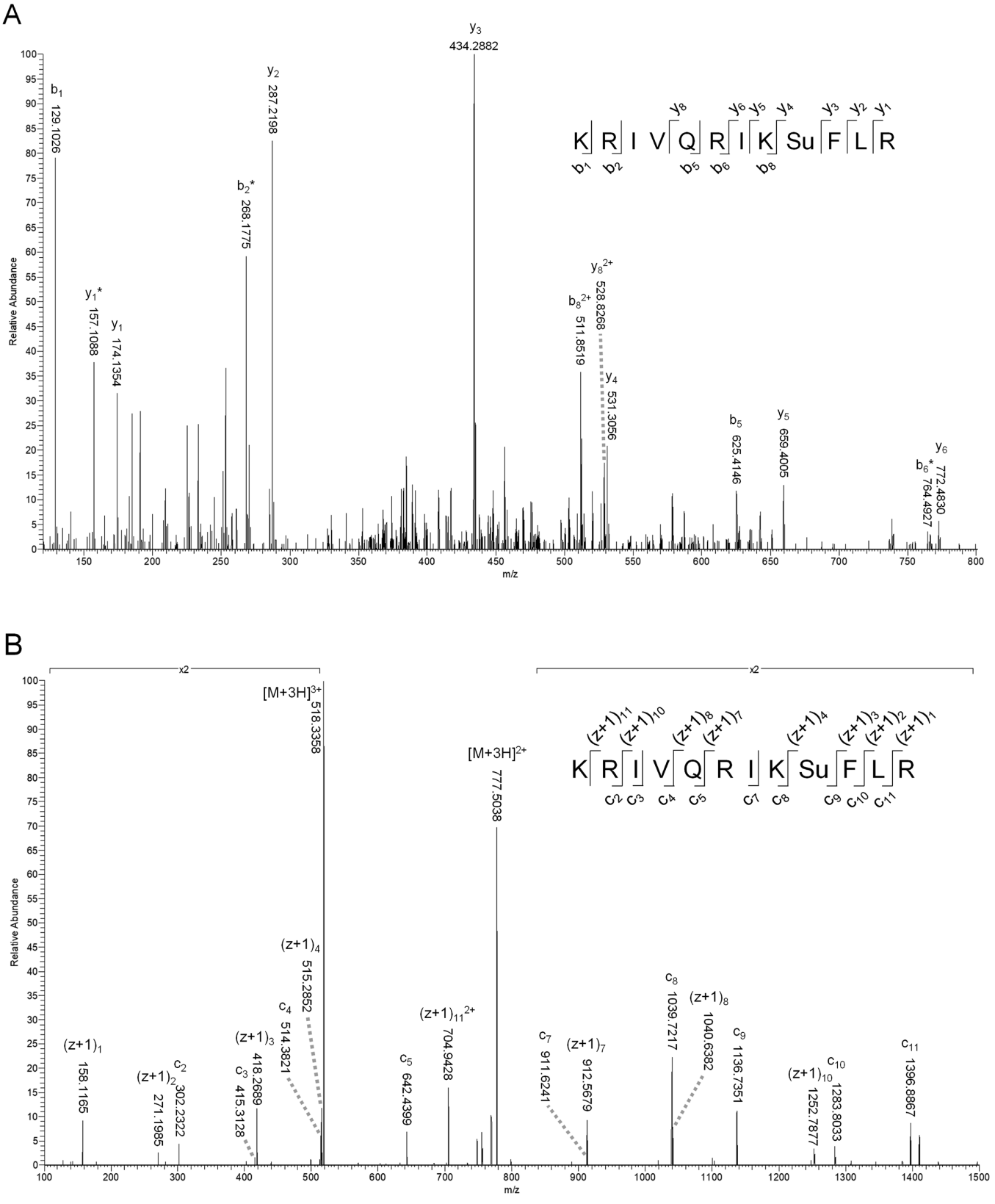

Figure 2. MS/MS spectra of KR12C by (A) HCD and (B) ETD fragmentation. Su denotes succinimide. The asterisk (*) indicates the loss of ammonia.

cells.[37−39] Cancer cells are more susceptible to cationic AMP targeting due to more negatively charged membranes of cancer cells than normal cells.[40] Previous studies have shown that LL37 exhibits cytotoxicity against the human colon cancer cell line HCT116 and the adult T leukemia cell Jurkat.[41,42] We tested the cytotoxic activity of the peptides against these two cell lines. Consistent with previous reports, LL37 significantly reduced the viability of two cell lines, while none of KR12 and

https://dx.doi.org/10.1021/acsomega.0c05503
ACS Omega 2021, 6, 4708−4718

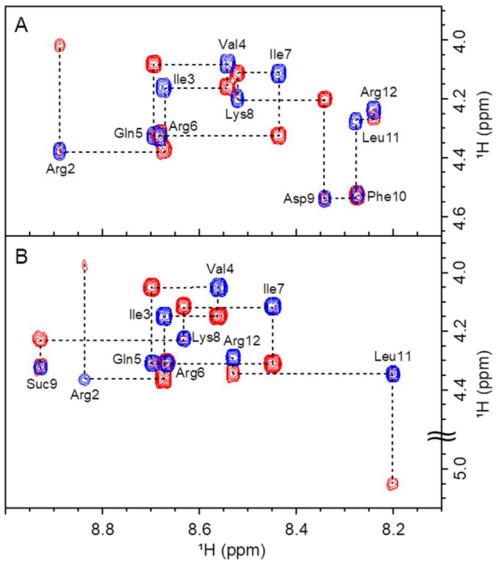

Figure 3. NOE sequential assignment of KR12 and KR12C. Shown are the HN-Hα regions of TOCSY (blue) and NOESY (red) spectra for (A) KR12 and (B) KR12C at 5 °C. Residues are labeled at the positions of the intraresidual HN-Hα peaks, and the inter-residual HN-Hα NOE connectivities are linked by dashed lines.

KR12C exhibited cytotoxic activities on two cell lines even at a concentration up to 80 μM (Figure 6A,B). The observation agrees with previous studies showing the selective toxicity of KR12 toward bacteria but not human cells.[26,43] The loss of cytotoxicity is mainly caused by the reduction in surface hydrophobicity, resulting in reduced membrane binding affinity of the peptide.[37] Since KR12C is less hydrophobic than KR12 as indicated by the retention times on RP-HPLC (Figure 1B), its membrane binding affinity may be lower than KR12. In addition, the difference of cytotoxic activity may be partly explained by the instability of KR12 and KR12C in the serum in comparison with LL37 (Figure 6C). After 15 min of incubation in 25% of serum, only ~25% of KR12 could be detected, while the level of LL37 was comparable to the 0 min control. The result of instability of KR12 in serum is consistent with a previous report.[35] In addition, the stability of KR12C was lower than that of KR12, as only ~5% of KR12C could be detected under the same condition. Taken together, the results indicate that neither of KR12 and KR12C exerts cytotoxic effects toward cancer cells and the loss of activity as compared to LL37 may be related to the reduction in surface hydrophobicity and the instability in serum.

DMTMM-Mediated Pyroglutamate Formation. Besides Asp/Asn, intraresidue cyclization can take place at Glu/Gln residues, especially for N-terminal Glu/Gln, which results in the formation of pyroglutamate (pGlu).[44] The formation of

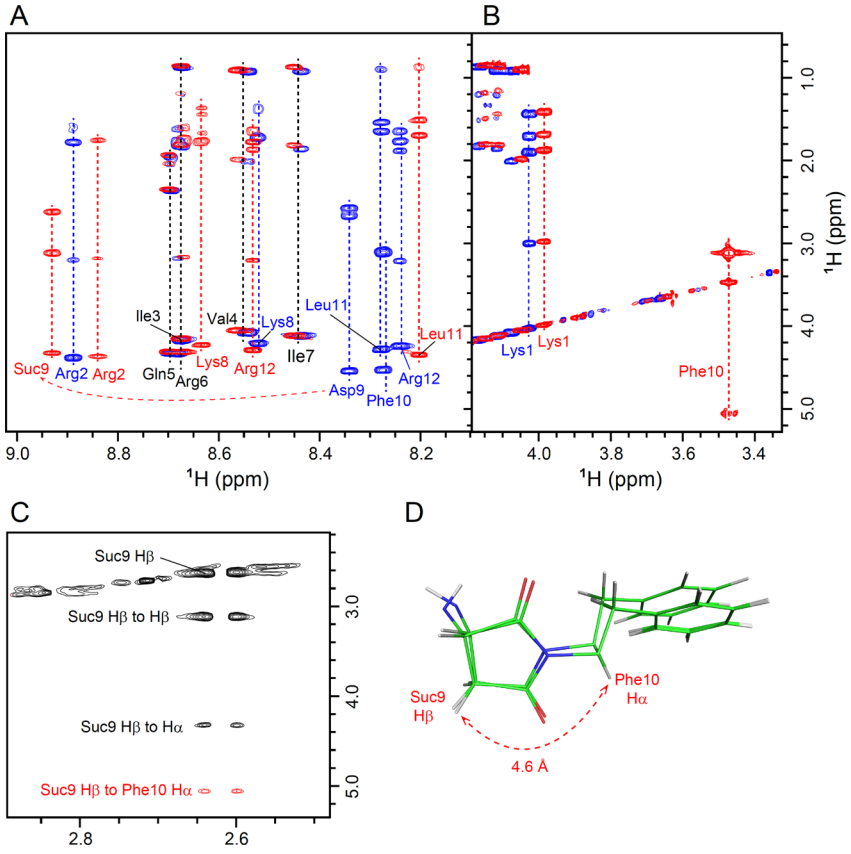

Figure 4. NMR results confirm the formation of Suc. (A) Fingerprint region (HN-to-aliphatic protons) on the TOCSY spectra of KR12 (blue peaks) and KR12C (red peaks). The residues from Ile3 to Ile7 show very similar peaks in both KR12 and KR12C and are indicated with black lines and labels. The TOCSY signals of Lys1 in both peptides and Phe10 in KR12C are shown in (B) owing to the lack of HN resonances. (C) Selected region of the NOESY spectra of KR12C showing clearly the NOE between Hα of Phe10 and Hβ of Suc9 (labeled and colored in red). (D) Final five KR12C structures calculated based on all the identified NOE peaks show that due to the formation of Suc, the distance between Hα of Phe10 and Hβ of Suc9 is around 4.6 Å.

https://dx.doi.org/10.1021/acsomega.0c05503
ACS Omega 2021, 6, 4708−4718

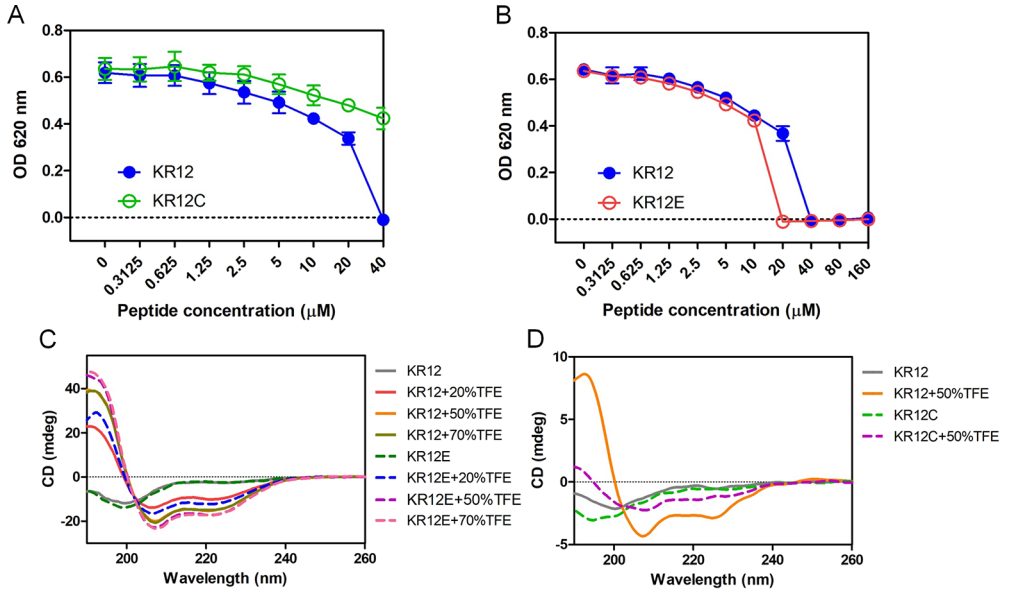

Figure 5. Relationships of antimicrobial activity and peptide helicity. Antimicrobial activity of (A) KR12C and (B) KR12E against *E. coli*. The data represent mean ± SD from three independent experiments. (C) CD spectra of KR12 (solid lines) and KR12E (dotted lines) using different concentrations of TFE. (D) CD spectra of KR12 (solid lines) and KR12C (dotted lines) in the absence or presence of 50% TFE. The spectra are expressed in absolute values of ellipticity in millidegrees (mdeg).

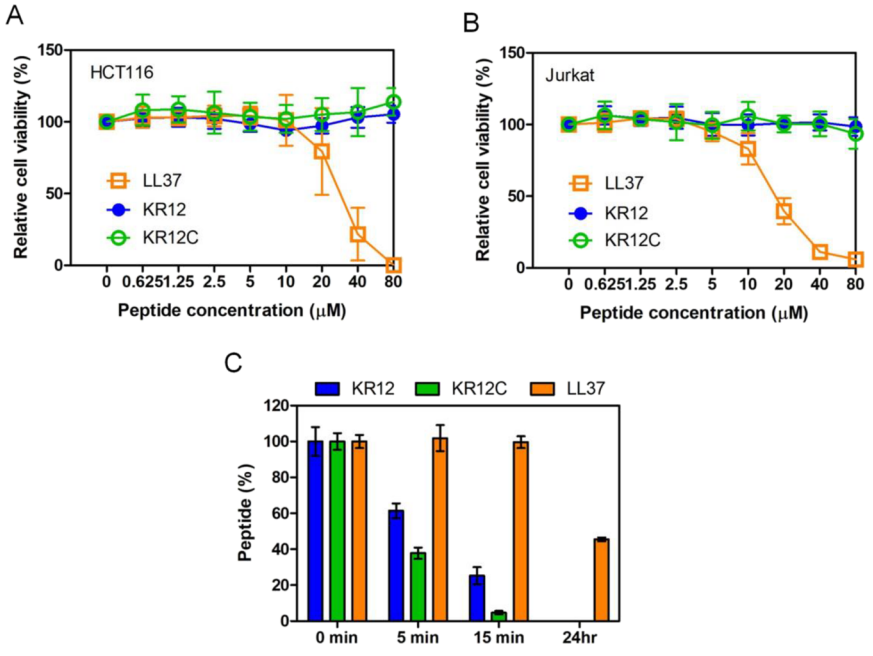

Figure 6. Cytotoxicity and serum stability of the peptides. Cytotoxicity of the peptides against (A) HCT116 and (B) Jurkat cells. (C) Peptides were incubated with 25% human serum for several time points at 37 °C. All data represent mean ± SD from three independent experiments.

pGlu is not only a spontaneous reaction, but it can also be catalyzed by glutaminyl cyclases.[45] Here, we tested whether DMTMM can mediate the formation of pGlu from N-terminal Glu/Gln by using the fluorescence probes, H-X-β-naphthylamine (X = Asp, Asn, Glu, and Gln; NA, naphthylamine). The fluorescence of β-naphthylamine can be enhanced when pGlu is formed and removed by pyroglutamyl aminopeptidase I.[46] After the reaction, the result showed that DMTMM was only able to mediate the formation of pGlu from Glu but not Gln (Figure 7A). The groups with the fluorescence probes, H-Asp/Asn-β-NA, served as negative controls. The pGlu-containing probe formed after the reaction can be clearly distinguished from the Glu-containing probe on the chromatogram (Figure 7B). The minor peak that occurred at a retention time of ∼16.5 min represented H-pGlu-β-NA containing the triazine part of DMTMM (∼139 Da) based on mass spectrometry analysis (Figure 7B and Figure S3). This may be due to an excess of DMTMM used in the reactions, which reacts with the amine groups, though the tendency for DMTMM to react with the amine groups is much lower than that with the carboxy groups. The reactions became predominant when there were no carboxy groups such as H-Asn/Gln-β-NA (Figure 7C,F and Figure S4). For the reaction with H-Asp-β-NA, the peak that occurred at a retention time of ∼16.9 min represented the

https://dx.doi.org/10.1021/acsomega.0c05503
ACS Omega 2021, 6, 4708−4718

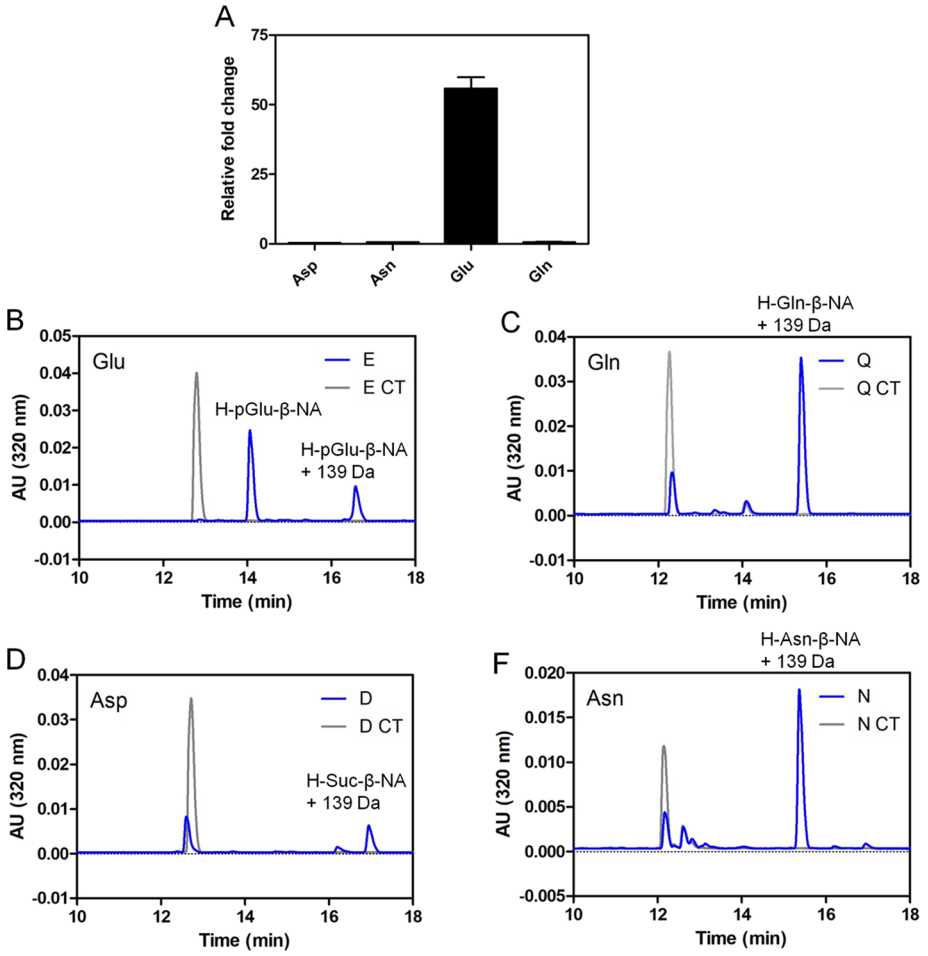

Figure 7. DMTMM-mediated pGlu formation. (A) Related fold changes of the fluorescence intensity produced by different substrates. RP-HPLC analysis of the mixtures obtained after the DMTMM reactions containing (B) H-Glu-*β*-NA, (C) H-Gln-*β*-NA, (D) H-Asp-*β*-NA, and (F) H-Asn-*β*-NA. CT denotes the control reaction that contains only the indicated fluorescence probe.

cyclized form with the triazine part of DMTMM (Figure 7D and Figure S4). Taken together, it is evident from the results that DMTMM can also be used for cyclization of N-terminal Glu to form pGlu.

CONCLUSIONS

Chemical modification of peptides/proteins has emerged as a powerful approach to improve the efficacy of biopharmaceuticals, whereas attention must be paid when the undesired modifications take place during storage and usage. In this study, we demonstrated that DMTMM can be used for intramolecular cyclization of acidic residues, Asp and Glu, resulting in the formation of Suc and pGlu, respectively. The formation of Suc in KR12 affected its helix-forming capability, which correlated with decreased antimicrobial activity. The modification is a common occurrence during the storage of biopharmaceuticals, leading to the product heterogeneity. It often induces structural changes and may have detrimental effects on the therapeutic efficacy and safety of a drug product. Thus, characterization of Suc in mABs in terms of its localization and function is important during pharmaceutical development. Our work provides a convenient and efficient method to produce Suc- or pGlu-containing peptides/proteins, which are useful tools for identification of the modifications and for studying their effects on peptide/protein function. Moreover, the method can be applied in designing biopharmaceuticals depending on the mechanism of action.

EXPERIMENTAL PROCEDURES

Peptides. The peptide KR12 (KRIVQRIKDFLR-NH2), KR12E (KRIVQRIKEFLR-NH2), and LL37 (LLGDFFRKSKEKIGKEFKRIVQRIKDFLRNLVPRTES) were synthesized by the peptide synthesis facility in the Institute of Biological Chemistry, Academia Sinica. The purity of the peptides was determined to be ≥95% based on RP-HPLC and MALDI-TOF/TOF-MS.

DMTMM Reactions. For preparation of Man-KR12, KR12 (5 mg, 3.2 μmol) was mixed with 4-aminophenyl α-D-manopyranoside (8.7 mg, 0.032 mmol) and then DMTMM (17.7 mg, 0.064 mmol) was added to the mixture in PBS (pH 7.4) in a final volume of 1.5 mL. For preparation of KR12C, KR12 (12 mg, 7.6 μmol) was mixed with DMTMM (42.48 mg, 0.15 mmol) in PBS (pH 7.4) in a final volume of 1.8 mL. The reaction mixtures were incubated with shaking at 250 rpm at 37 °C for 3 h. After the reaction, the samples were added to Pierce peptide desalting spin columns (Thermo Fisher Scientific, 89851) and were eluted according to the manufacturer's instruction. The eluates were analyzed by RP-HPLC and MALDI-TOF/TOF-MS. The fractions containing the pure peptide were collected and then freeze-dried.

https://dx.doi.org/10.1021/acsomega.0c05503
ACS Omega 2021, 6, 4708−4718

For cyclization of H-X-β-NA (X = Asp, Asn, Glu, and Gln; NA, naphthylamine; BACHEM, 4002834, 4007065, 4001467, and 4001674), X-β-NA (0.5 mM) was mixed with DMTMM (50 mM) in 100 μL of 50 mM HEPES-NaOH (pH 7.5). The reaction mixtures were incubated with shaking at 250 rpm at 37 °C for 3 h. After the reaction, the samples were added 1 μL of 10% trifluoroacetic acid (TFA) and evaluated by RP-HPLC.

RP-HPLC Analysis and Purification. After the reactions, the peptides were analyzed and purified by RP-HPLC on a C18 column (XBridge Peptide BEH C18 Column 300 Å, 5 μm, 4.6 mm × 100 mm) using a Waters module W2690/5 and a PDA detector W2998 at a flow rate of 1.0 mL/min with detection at 214 or 320 nm. The mobile phase included water with 0.1% TFA for solvent A and acetonitrile (ACN) with 0.1% TFA for solvent B. Peaks were collected and identified by mass spectrometry.

Antimicrobial Activity Assay. *E. coli* (ATCC 25922) were grown in Mueller-Hinton broth at 37 °C until OD_{600} reached 0.3 with a density of approximately 1×10^8 CFU/mL. The peptides were serially two-fold diluted in water with a starting concentration of 400 μM or 1600 μM to 3.125 μM as indicated. A total of 10 μL of diluted peptides was added to 90 μL of the 10^4-fold diluted bacterial cultures in 96-well plates (Corning, CLS-3879). After incubation with shaking at 180 rpm at 37 °C for 15 h, bacterial growth was assessed by measuring the absorbance at 620 nm in a BioTek Synergy H1 microplate reader. MIC is determined as the lowest peptide concentration at which the peptide completely inhibits the growth of the bacteria.

Liquid Chromatography Tandem Mass Spectrometry (LC−MS/MS) Analysis. NanoLC−nanoESI-MS/MS analysis was performed on a nanoAcquity system (Waters, Milford, MA) connected to the Orbitrap hybrid series mass spectrometer (Thermo Electron, Bremen, Germany) equipped with a PicoView nanospray interface (New Objective, Woburn, MA). Peptide mixtures were loaded onto a 75 μm-ID, 25 cm-length C18 BEH column (Waters, Milford, MA) packed with 1.7 μm particles with a pore with of 130 Å and were separated using a segmented gradient in 30 min from 5% to 35% solvent B (acetonitrile with 0.1% formic acid) at a flow rate of 300 nL/min and a column temperature of 35 °C. Solvent A was 0.1% formic acid in water. The mass spectrometer was operated in data-dependent mode. ETD fragmentation was performed on an Orbitrap Elite hybrid mass spectrometer; survey full scan MS spectra were acquired in the orbitrap (m/z 300−1600) with the resolution set to 60 K at m/z 400 and automatic gain control (AGC) target at 10^6. The 15 most intense ions were sequentially isolated for MS/MS fragmentation and detection in the orbitrap. For MS/MS, we used a resolution of 15,000, an isolation window of 2 m/z, and a target value of 50,000 ions, with maximum accumulation times of 200 ms. The fluoranthene reaction time was set to 100 ms. Ions with a single and unrecognized charge state were also excluded. StepHCD fragmentation was performed on an LTQ Orbitrap Velos hybrid mass spectrometer; survey full scan MS spectra were acquired in the orbitrap (m/z 300−2000) with the resolution set to 60 K at m/z 400 and automatic gain control (AGC) target at 10^6. The 10 most intense ions were sequentially isolated for MS/MS fragmentation and detection in the orbitrap. For MS/MS, we used a resolution of 7500, an isolation window of 2 m/z, and a target value of 50,000 ions, with maximum accumulation times of 250 ms. Fragmentation was performed with normalized collision energies of 65%, 70%, and 75% with an activation time of 0.1 ms. Ions with a single and unrecognized charge state were also excluded.

The MS and MS/MS raw data were converted to Mascot Generic Files (MGF) using Proteome Discoverer (v2.4.0.305; Thermo Scientific) and searched against customized database containing a single peptide sequence with the Mascot Daemon server (v.2.7.0; Matrix Science). Search criteria used were NoCleave digestion, with variable modifications set as amidated (C-term), dehydrated (D), a mass accuracy of 10 ppm for the parent ion, and 0.02 Da for the fragment ions.

NMR Spectroscopy. All NMR experiments were acquired on a Bruker AVANCE III HD 600 MHz spectrometer with a BBFO 5 mm probe head. Samples were dissolved in 0.25 mL of H_2O/D_2O (9:1) to a concentration of 0.2 mM and placed in BMS005B SHIGEMI tubes. 2D TOCSY, NOESY, and DQF-COSY spectra were collected into 2048 points in t2 dimension and 256 points in t1 dimension with a relaxation delay of 2 s at 278 K. The TOCSY spectra were recorded using the DIPSI2 pulse sequence with mixing times of 75 ms, and 400 ms mixing times were used for NOESY spectra. All NMR spectra were processed and analyzed using Topspin 3.6 (Buker Biospin), referenced to 2,2-dimethyl-2-silapentane-5-sulfonate (DSS). Complete ^{1}H resonance assignments of KR12 and KR12C are listed in Tables S1 and S2, respectively.

NMR structures were calculated from mainly NOE restraints using the program XPLOR-NIH 3.0.[47] Simulated annealing was performed using 6000 steps at 1000 K and 20,000 steps by gradually cooling the temperature to 100 K. Also, the structures were energy-minimized using 500 steps of Powell energy minimization. The final 50 contained no NOE distance constraint violations greater than 0.3 Å. From these, a family of five was chosen based on their total energy.

Circular Dichroism (CD). CD spectra were measured at 25 °C on a J-815 Spectrometer (JASCO) using a 1 mm path length quartz cell. A 100 or 20 μM peptide was prepared in 10 mM sodium phosphate buffer and in the absence or presence of indicated concentration of TFE. The spectra were recorded between 190 and 260 nm wavelength with a data pitch of 0.5 nm and bandwidth of 1 nm and with four accumulations at a scanning speed of 50 nm/min.

Viability Assay for Mammalian Cells. HCT116 cells (ATCC, CCL-247) were maintained in McCoy's 5A modified medium (Gibco, 16600082) with 10% heat-inactivated fetal bovine serum (HI-FBS; Gibco, A3840102). Jurkat cells (ATCC, TIB-152) were maintained in RPMI-1640 medium (Gibco, A10491) with 10% HI-FBS. All cells were cultured under 5% CO_2 at 37 °C. Cells were seeded in 96-well plates at a density of 5000 cells/well in 100 μL of medium. After 24 h of incubation, cells were treated with serially two-fold diluted peptides with a starting concentration of 80 μM and incubated for another 48 h. CellTiter-Glo Luminescent Cell Viability Assay (Promega, G7570) was used to determine the cell viability based on the manufacturer's instruction.

Peptide Stability in Human Serum. RP-HPLC was used to determine the stability of the peptides in human serum.[48] Human serum (Sigma-Aldrich, H4522) was centrifuged at 13000 rpm for 10 min to remove lipids before use. The peptides were mixed with a solution of 25% human serum in PBS to get a final concentration of 50 μM in a 30 μL reaction volume. The peptides with serum were incubated at 37 °C with shaking at 250 rpm, and the reaction was stopped at the desired time point by adding 60 μL of ACN with 2% TFA and incubated on ice for 10 min to precipitate serum proteins. The

https://dx.doi.org/10.1021/acsomega.0c05503
ACS Omega 2021, 6, 4708−4718

samples then were centrifuged at 13000 rpm for 20 min at 4 °C. A total of 60 μL of the supernatant was taken and added to 120 μL of 0.1% TFA. The samples were analyzed by RP-HPLC, and the amounts of the peptides remaining were quantified by their peak areas. The percentage was calculated by comparing the peak area of the peptide remaining at each time point to time zero. The data were obtained from three independent experiments.

Pyroglutamate Detection. To detect the formation of pyroglutamate after the DMTMM reactions, 20 μL of the reaction mixtures containing the substrates H-X-β-NA was added into 60 μL of 50 mM HEPES-NaOH (pH 7.5) and 20 μL of human pyroglutamyl aminopeptidase I (1.6 mg/mL) was added in a 96-well plate. Fluorescence at excitation 320 nm and emission 410 nm was measured at 25 °C using a BioTek Synergy H4 Hybrid Microplate Reader. The relative fold changes were calculated by dividing the values from the experimental groups (H-X-β-NA + DMTMM) by the values from the control groups (H-X-β-NA only).

■ ASSOCIATED CONTENT

Supporting Information

The Supporting Information is available free of charge at https://pubs.acs.org/doi/10.1021/acsomega.0c05503.

(Figure S1) Conjugation scheme of Man-KR12, (Figure S2) mass spectra of Man-KR12 and KR12C, (Figure S3) mass spectra of H-pGlu-β-NA and H-pGlu-β-NA + 139 Da, (Figure S4) mass spectra of H-Gln-β-NA + 139 Da, H-Suc-β-NA + 139 Da, and H-Asn-β-NA + 139 Da, (Table S1) ^{1}H chemical shift assignments of KR12 at 278 K, and (Table S2) ^{1}H chemical shift assignment of KR12C at 278 K (PDF)

■ AUTHOR INFORMATION

Corresponding Author

Andrew H.-J. Wang − *Institute of Biological Chemistry, Academia Sinica, Taipei 115, Taiwan;* orcid.org/0000-0002-0016-5337; Phone: (8862)-2788-1981; Email: ahjwang@gate.sinica.edu.tw; Fax: (8862)-2788-2043

Authors

Chi-Hua Lee − *Institute of Biological Chemistry, Academia Sinica, Taipei 115, Taiwan;* orcid.org/0000-0002-9292-9639

Yuan-Chao Lou − *Biomedical Translation Research Center, Academia Sinica, Taipei 115, Taiwan*

Complete contact information is available at: https://pubs.acs.org/10.1021/acsomega.0c05503

Notes

The authors declare no competing financial interest.

■ ACKNOWLEDGMENTS

We are grateful to Dr. Long-Sen Chang from National Sun Yat-Sen University for his important considerations and suggestions for peptide/protein mannosylation. We thank Yu-Ling Hwang of the Institute of Biological Chemistry for the peptide synthesis. We thank Cheng-Hsilin Hsieh for technical assistance in MALDI-TOF/TOF mass spectrometry from the Genomics Core at the Institute of Molecular Biology. Orbitrap hybrid series data were acquired at the Academia Sinica Common Mass Spectrometry Facilities for Proteomics and Protein Modification Analysis located at the Institute of Biological Chemistry, Academia Sinica, supported by Academia Sinica Core Facility and Innovative Instrument Project (AS-CFII-108-107). We thank the NMR Core Facility of the National Biotechnology Research Park (NBRP), funded by NBRP Core Facility Service Project (AS-NBRP-CF-109-102-3) of Academia Sinica, for the technical support in NMR spectra. This work was supported by the Program for Translational Innovation of Biopharmaceutical Development-Technology Supporting Platform Axis.

■ ABBREVIATIONS

DMTMM 4-(4,6-dimethoxy-1,3,5-triazin-2-yl)-4-methylmorpholinium chloride
AMP antimicrobial peptide
Suc succinimide
mAbs recombinant monoclonal antibodies
LC−MS/MS liquid chromatography tandem mass spectrometry
NMR nuclear magnetic resonance
Man 4-aminophenyl-α-D-mannopyranoside
RP-HPLC reversed-phase high-performance liquid chromatography
MALDI-TOF/TOF-MS matrix-assisted laser desorption/ionization time-of-flight/time-of-flight mass spectrometry
MW molecular weight
MIC minimum inhibitory concentration
HCD higher-energy collisional dissociation
ETD electron transfer dissociation
TFE 2,2,2-trifluoroethanol
NA naphthylamine
TFA trifluoroacetic acid
CD circular dichroism

■ REFERENCES

(1) Aggarwal, S. R. What's fueling the biotech engine-2012 to 2013. *Nat. Biotechnol.* **2014**, *32*, 32−39.
(2) van Witteloostuijn, S. B.; Pedersen, S. L.; Jensen, K. J. Half-life extension of biopharmaceuticals using chemical methods: alternatives to PEGylation. *ChemMedChem* **2016**, *11*, 2474−2495.
(3) Grassi, L.; Cabrele, C. Susceptibility of protein therapeutics to spontaneous chemical modifications by oxidation, cyclization, and elimination reactions. *Amino Acids* **2019**, *51*, 1409−1431.
(4) Geiger, T.; Clarke, S. Deamidation, isomerization, and racemization at asparaginyl and aspartyl residues in peptides. Succinimide-linked reactions that contribute to protein degradation. *J. Biol. Chem.* **1987**, *262*, 785−794.
(5) Cacia, J.; Keck, R.; Presta, L. G.; Frenz, J. Isomerization of an aspartic acid residue in the complementarity-determining regions of a recombinant antibody to human IgE: identification and effect on binding affinity. *Biochemistry* **1996**, *35*, 1897−1903.
(6) Huang, L.; Lu, J.; Wroblewski, V. J.; Beals, J. M.; Riggin, R. M. In vivo deamidation characterization of monoclonal antibody by LC/MS/MS. *Anal. Chem.* **2005**, *77*, 1432−1439.
(7) Yan, B.; Steen, S.; Hambly, D.; Valliere-Douglass, J.; Vanden Bos, T.; Smallwood, S.; Yates, Z.; Arroll, T.; Han, Y.; Gadgil, H.; Latypov, R. F.; Wallace, A.; Lim, A.; Kleemann, G. R.; Wang, W.; Balland, A. Succinimide formation at Asn 55 in the complementarity determining region of a recombinant monoclonal antibody IgG1 heavy chain. *J. Pharm. Sci.* **2009**, *98*, 3509−3521.
(8) Shimizu, T.; Watanabe, A.; Ogawara, M.; Mori, H.; Shirasawa, T. Isoaspartate formation and neurodegeneration in Alzheimer's disease. *Arch. Biochem. Biophys.* **2000**, *381*, 225−234.

(9) Fujii, N.; Sakaue, H.; Sasaki, H.; Fujii, N. A rapid, comprehensive liquid chromatography-mass spectrometry (LC-MS)-based survey of the Asp isomers in crystallins from human cataract lenses. *J. Biol. Chem.* **2012**, *287*, 39992−40002.
(10) Chu, G. C.; Chelius, D.; Xiao, G.; Khor, H. K.; Coulibaly, S.; Bondarenko, P. V. Accumulation of succinimide in a recombinant monoclonal antibody in mildly acidic buffers under elevated temperatures. *Pharm. Res.* **2007**, *24*, 1145−1156.
(11) Ouellette, D.; Chumsae, C.; Clabbers, A.; Radziejewski, C.; Correia, I. Comparison of the in vitro and in vivo stability of a succinimide intermediate observed on a therapeutic IgG1 molecule. *mAbs* **2013**, *5*, 432−444.
(12) Kumar, S.; Prakash, S.; Gupta, K.; Dongre, A.; Balaram, P.; Balaram, H. Unexpected functional implication of a stable succinimide in the structural stability of Methanocaldococcus jannaschii glutaminase. *Nat. Commun.* **2016**, *7*, 12798.
(13) Xu, M. Q.; Comb, D. G.; Paulus, H.; Noren, C. J.; Shao, Y.; Perler, F. B. Protein splicing: an analysis of the branched intermediate and its resolution by succinimide formation. *EMBO J.* **1994**, *13*, 5517−5522.
(14) Catak, S.; Monard, G.; Aviyente, V.; Ruiz-López, M. F. Deamidation of asparagine residues: direct hydrolysis versus succinimide-mediated deamidation mechanisms. *J. Phys. Chem. A* **2009**, *113*, 1111−1120.
(15) Konuklar, F. A. S.; Aviyente, V. Modelling the hydrolysis of succinimide: formation of aspartate and reversible isomerization of aspartic acid via succinimide. *Org. Biomol. Chem.* **2003**, *1*, 2290−2297.
(16) Grassi, L.; Regl, C.; Wildner, S.; Gadermaier, G.; Huber, C. G.; Cabrele, C.; Schubert, M. Complete NMR assignment of succinimide and its detection and quantification in peptides and intact proteins. *Anal. Chem.* **2017**, *89*, 11962−11970.
(17) Aki, K.; Fujii, N.; Fujii, N. Kinetics of isomerization and inversion of aspartate 58 of αA-crystallin peptide mimics under physiological conditions. *PLoS One* **2013**, *8*, No. e58515.
(18) Nowak, C.; Ponniah, G.; Neill, A.; Liu, H. Characterization of succinimide stability during trypsin digestion for LC-MS analysis. *Anal. Biochem.* **2017**, *526*, 1−8.
(19) Cao, M.; Mulagapati, S. H. R.; Vemulapalli, B.; Wang, J.; Saveliev, S. V.; Urh, M.; Hunter, A.; Liu, D. Characterization and quantification of succinimide using peptide mapping under low-pH conditions and hydrophobic interaction chromatography. *Anal. Biochem.* **2019**, *566*, 151−159.
(20) Cao, M.; Xu, W.; Niu, B.; Kabundi, I.; Luo, H.; Prophet, M.; Chen, W.; Liu, D.; Saveliev, S. V.; Urh, M.; Wang, J. An automated and qualified platform method for site-specific succinimide and deamidation quantitation using low-pH peptide mapping. *J. Pharm. Sci.* **2019**, *108*, 3540−3549.
(21) Friedrich, M. G.; Wang, Z.; Schey, K. L.; Truscott, R. J. W. Spontaneous cross-linking of proteins at aspartate and asparagine residues is mediated via a succinimide intermediate. *Biochem. J.* **2018**, *475*, 3189−3200.
(22) Mahlapuu, M.; Håkansson, J.; Ringstad, L.; Björn, C. Antimicrobial peptides: an emerging category of therapeutic agents. *Front. Cell Infect. Microbiol.* **2016**, *6*, 194.
(23) Yeaman, M. R.; Yount, N. Y. Mechanisms of antimicrobial peptide action and resistance. *Pharmacol. Rev.* **2003**, *55*, 27−55.
(24) Gudmundsson, G. H.; Agerberth, B.; Odeberg, J.; Bergman, T.; Olsson, B.; Salcedo, R. The human gene FALL39 and processing of the cathelin precursor to the antibacterial peptide LL-37 in granulocytes. *Eur. J. Biochem.* **1996**, *238*, 325−332.
(25) Johansson, J.; Gudmundsson, G. H.; Rottenberg, M. E.; Berndt, K. D.; Agerberth, B. Conformation-dependent antibacterial activity of the naturally occurring human peptide LL-37. *J. Biol. Chem.* **1998**, *273*, 3718−3724.
(26) Wang, G. Structures of human host defense cathelicidin LL-37 and its smallest antimicrobial peptide KR-12 in lipid micelles. *J. Biol. Chem.* **2008**, *283*, 32637−32643.
(27) Kunishima, M.; Kawachi, C.; Monta, J.; Terao, K.; Iwasaki, F.; Tani, S. 4-(4,6-dimethoxy-1,3,5-triazin-2-yl)-4-methyl-morpholinium chloride: an efficient condensing agent leading to the formation of amides and esters. *Tetrahedron* **1999**, *55*, 13159−13170.
(28) Perez-Garmendia, R.; Gevorkian, G. Pyroglutamate-modified amyloid beta peptides: emerging targets for Alzheimer's disease immunotherapy. *Curr. Neuropharmacol.* **2013**, *11*, 491−498.
(29) Liu, Y. D.; Goetze, A. M.; Bass, R. B.; Flynn, G. C. N-terminal glutamate to pyroglutamate conversion in vivo for human IgG2 antibodies. *J. Biol. Chem.* **2011**, *286*, 11211−11217.
(30) Tang, C.-C.; Shi, Y.-J.; Chen, Y.-J.; Chang, L.-S. Ovalbumin with glycated carboxyl groups shows membrane-damaging activity. *Int. J. Mol. Sci.* **2017**, *18*, 520.
(31) Tsai, C.-Y.; Chen, Y.-J.; Fu, Y.-S.; Chang, L.-S. Antibacterial and membrane-damaging activities of mannosylated bovine serum albumin. *Arch. Biochem. Biophys.* **2015**, *573*, 14−22.
(32) Mishra, B.; Epand, R. F.; Epand, R. M.; Wang, G. Structural location determines functional roles of the basic amino acids of KR-12, the smallest antimicrobial peptide from human cathelicidin LL-37. *RSC Adv.* **2013**, 19560.
(33) Wüthrich, K. *NMR of Protein and Nucleic Acids*; Wiley: New York, 1986.
(34) Nguyen, L. T.; Haney, E. F.; Vogel, H. J. The expanding scope of antimicrobial peptide structures and their modes of action. *Trends Biotechnol.* **2011**, *29*, 464−472.
(35) Gunasekera, S.; Muhammad, T.; Strömstedt, A. A.; Rosengren, K. J.; Göransson, U. Alanine and lysine scans of the LL-37-derived peptide fragment KR-12 reveal key residues for antimicrobial activity. *ChemBioChem* **2018**, *19*, 931−939.
(36) Johnson, W. C., Jr. Protein secondary structure and circular dichroism: a practical guide. *Proteins* **1990**, *7*, 205−214.
(37) Li, X.; Li, Y.; Han, H.; Miller, D. W.; Wang, G. Solution structures of human LL-37 fragments and NMR-based identification of a minimal membrane-targeting antimicrobial and anticancer region. *J. Am. Chem. Soc.* **2006**, *128*, 5776−5785.
(38) Thomas, A. J.; Pulsipher, A.; Davis, B. M.; Alt, J. A. LL-37 causes cell death of human nasal epithelial cells, which is inhibited with a synthetic glycosaminoglycan. *PLoS One* **2017**, *12*, No. e0183542.
(39) Scheenstra, M. R.; van den Belt, M.; Tjeerdsma-van Bokhoven, J. L. M.; Schneider, V. A. F.; Ordonez, S. R.; van Dijk, A.; Veldhuizen, E. J. A.; Haagsman, H. P. Cathelicidins PMAP-36, LL-37 and CATH-2 are similar peptides with different modes of action. *Sci. Rep.* **2019**, *9*, 4780.
(40) Schweizer, F. Cationic amphiphilic peptides with cancer-selective toxicity. *Eur. J. Pharmacol.* **2009**, *625*, 190−194.
(41) Ren, S. X.; Shen, J.; Cheng, A. S. L.; Lu, L.; Chan, R. L. Y.; Li, Z. J.; Wang, X. J.; Wong, C. C. M.; Zhang, L.; Ng, S. S. M.; Chan, F. L.; Chan, F. K. L.; Yu, J.; Sung, J. J. Y.; Wu, W. K. K.; Cho, C. H. FK-16 derived from the anticancer peptide LL-37 induces caspase-independent apoptosis and autophagic cell death in colon cancer cells. *PLoS One* **2013**, *8*, No. e63641.
(42) Mader, J. S.; Mookherjee, N.; Hancock, R. E. W.; Bleackley, R. C. The human host defense peptide LL-37 induces apoptosis in a calpain- and apoptosis-inducing factor-dependent manner involving Bax activity. *Mol. Cancer Res.* **2009**, *7*, 689−702.
(43) Wang, G.; Watson, K. M.; Buckheit, R. W., Jr. Anti-human immunodeficiency virus type 1 activities of antimicrobial peptides derived from human and bovine cathelicidins. *Antimicrob. Agents Chemother.* **2008**, *52*, 3438−3440.
(44) Messer, M.; Ottesen, M. Isolation and properties of glutamine cyclotransferase of dried papaya latex. *Biochim. Biophys. Acta, Spec. Sect. Enzymol. Subj.* **1965**, *35*, 1−24.
(45) Huang, K.-F.; Liu, Y.-L.; Cheng, W.-J.; Ko, T.-P.; Wang, A. H.-J. Crystal structures of human glutaminyl cyclase, an enzyme responsible for protein N-terminal pyroglutamate formation. *Proc. Natl. Acad. Sci. U. S. A.* **2005**, *102*, 13117−13122.
(46) Schilling, S.; Hoffmann, T.; Wermann, M.; Heiser, U.; Wasternack, C.; Demuth, H.-U. Continuous spectrometric assays for glutaminyl cyclase activity. *Anal. Biochem.* **2002**, *303*, 49−56.

https://dx.doi.org/10.1021/acsomega.0c05503
ACS Omega 2021, 6, 4708−4718

(47) Schwieters, C. D.; Kuszewski, J. J.; Clore, G. M. Using Xplor–NIH. for NMR molecular structure determination. *Prog. Nucl. Magn. Reson. Spectrosc.* **2006**, *48*, 47–62.
(48) Lawrence, N.; Dennis, A. S. M.; Lehane, A. M.; Ehmann, A.; Harvey, P. J.; Benfield, A. H.; Cheneval, O.; Henriques, S. T.; Craik, D. J.; McMorran, B. J. Defense peptides engineered from human platelet factor 4 kill plasmodium by selective membrane disruption. *Cell Chem. Biol.* **2018**, *25*, 1140–1150.e5.

https://dx.doi.org/10.1021/acsomega.0c05503
ACS Omega 2021, 6, 4708–4718